Proceedings of the 4th International Conference on Biological Engineering and Medical Science
DOI: 10.54254/2753-8818/59/20241372

Pioneering anti-inflammatory therapy: The path to precision therapy with C3aR peptide libraries

Megan Hsu

The Lawrenceville School, 2500 Main St, Lawrenceville, NJ 08648, USA

ltzumegan@gmail.com

Abstract. Inflammation, a pervasive process with profound implications for tissue, joint, and vascular health, underscores the critical importance of immune system regulation in maintaining bodily homeostasis. Central to this regulatory network is the complement system, a complex array of proteins that orchestrate immune responses to infections and cellular damage. Among these proteins, the complement component 3a receptor (C3aR) serves as a pivotal mediator, triggering inflammatory cascades upon binding to the anaphylatoxin C3a. Targeting C3aR has emerged as a promising strategy for anti-inflammatory therapy, driven by recent advances in structural biology elucidating the complex architecture of the C3a-C3aR interaction. This study focuses on the design of high-affinity peptides targeting the C3aR receptor, leveraging ligand design and docking techniques to optimize binding interactions. Utilizing computational tools with sophisticated algorithms, we modeled the binding affinity of mutated ligands with the C3aR receptor, providing insights into the potential efficacy of peptide-based therapeutics. Our findings reveal that mutations at residues G74 and A76 enhance the binding affinity of the ligand with the C3aR receptor, offering a promising avenue for the development of novel anti-inflammatory agents. By elucidating the molecular determinants underlying peptide-receptor interactions within the C3a system, this study advances our understanding of inflammation biology and lays the groundwork for the rational design of targeted therapeutics. These insights hold potential for the development of potent and selective C3aR agonists/antagonists, offering new avenues for the treatment of inflammatory diseases and enhancing patient outcomes.

Keywords: C3aR (complement component 3a receptor), Inflammation, Complement system, Peptide-based therapeutics.

1. Introduction

The complement system, comprising a cascade of proteins and receptors, is particularly noteworthy for its key role in coordinating inflammatory responses. The complement system operates as a complex network of proteins and receptors that collectively augment immune responses, with inflammation being a significant result of its activation [1, 2, 3]. Central to its function is the efficient amplification of immune responses, leading to the recruitment and activation of immune cells, opsonization of pathogens, and clearance of cellular debris. Notably, dysregulation of the complement system can result in chronic inflammation and contribute to the pathogenesis of various inflammatory diseases [4]. Among the receptors implicated in complement-mediated inflammation, the C3a receptor (C3aR) holds an important position. C3aR, a G-protein coupled receptor (GPCR), plays a critical role in modulating immune responses by binding to its ligand, C3a, and initiating downstream signaling cascades [2, 5].

DOI: 10.54254/2753-8818/59/20241372

Activation of C3aR triggers various cellular responses, including chemotaxis, degranulation, and cytokine production, thereby amplifying inflammatory processes and contributing to immune surveillance [6]. Upon binding of C3a to C3aR, a series of conformational changes occur, leading to the activation of intracellular signaling pathways. This activation culminates in the release of pro-inflammatory mediators, such as histamine and leukotrienes, and the recruitment of immune cells to sites of inflammation [7]. Thus, the interaction between C3a and C3aR serves as a critical checkpoint in the regulation of immune responses and inflammation. Given the central role of C3aR in inflammation, there has been considerable interest in developing pharmacological agents that modulate its activity.

Agonists and antagonists targeting C3aR offer potential therapeutic avenues for the management of inflammatory diseases by either enhancing or inhibiting its activity, respectively [8, 9, 10]. C3aR antagonists are pharmacological agents designed to block or inhibit the activity of the C3a receptor (C3aR), thereby interfering with the downstream signaling pathways triggered by C3a binding. By antagonizing C3aR, these compounds aim to mitigate excessive inflammation and modulate immune responses associated with various inflammatory and autoimmune diseases. C3aR agonists are compounds or molecules that bind to and activate the C3a receptor (C3aR), thereby triggering downstream signaling pathways and eliciting immune responses. These agonists mimic the action of the endogenous ligand, C3a, and can enhance inflammatory processes, immune cell recruitment, and cytokine production.

Efforts to identify and optimize C3aR agonists and antagonists have encompassed screening libraries of small molecules, peptides, and biologics to pinpoint compounds exhibiting agonistic or antagonistic activity. Structure-activity relationship studies and computational modeling approaches have played pivotal roles in refining the design of potent and selective C3aR modulators with enhanced pharmacokinetic properties. Recent advances [11, 12], including the elucidation of the C3a and C3aR complex structure through Cryo-Electron Microscopy (Cryo-EM), have provided invaluable insights, paving the way for the development of highly efficacious and selective C3aR agonists and antagonists.

In this study, we conducted a comprehensive analysis of the complex structure involving the C3aR receptor and its ligand C3a, whose role in the complement system was recently elucidated by a research group employing Cryo-Electron Microscopy (Cryo-EM) technology. Through meticulous examination of the protein complex's structure, we identified specific residues poised for alteration to enhance the peptide's efficacy as an antagonist or agonist for the C3aR receptor. These modifications aim to augment the receptor's anti-inflammatory functions within the immune system.

2. Material and Methods

2.1. Structure Retrieval and Preparation

The structure of both C3aR and C3a was retrieved from the Cryo-EM structure of the C3a-C3aR-Go complex, accessed through RCSB with accession number 8i9l from the Protein Data Bank (https://www.rcsb.org/). Specifically, C3aR was extracted from the complex as the receptor protein, while C3a was isolated from the 8i9l complex and utilized as a template for peptide design. Pymol (https://pymol.org/) served as the molecular visualization tool for rendering and animating the 3D molecular structures in this study.

2.2. Protein–Ligand Docking

To assess the binding of the C3a ligand to the C3aR receptor, molecular docking experiments were conducted to elucidate the interaction patterns between them. For this purpose, HDOCK (accessible via the HDock website) [13] was employed for docking simulations. HDOCK utilizes an iterative knowledge-based scoring function known as ITScore-PP to rank the top 10 poses, with more negative scores indicating stronger binding interactions between the two macromolecules. Subsequently, the resulting docking poses obtained from HDOCK were subjected to further analysis to discern specific interaction patterns between C3aR and C3a. The same procedure was followed for docking of selected single mutation or double mutation to the C3aR receptor.

DOI: 10.54254/2753-8818/59/20241372

2.3. Residue Scan to Design a Peptide Library

Utilizing small peptides derived from native sequences has been a common practice in designing short peptide derivatives. Previous studies [8, 11, 12] have indicated that the C-terminal domain of C3a, particularly the last 10 residues, plays a crucial role in binding to C3aR. Therefore, we constructed a wild-type peptide spanning residues 63 to 77 using C3a as a template. Subsequently, we manipulated these residues to design decoy peptides against C3aR using MOE (Molecular Operating Environment, https://www.chemcomp.com/Research-Citing_MOE.htm). Given the significance of key residues at the interface for mutant modeling, we employed a Residue Scanning strategy, where each residue was systematically replaced by the 19 other amino acids, to evaluate the impact of individual residues on the interaction with C3aR. This residue scanning approach generated a database of mutant peptides along with their respective scores.

Initially, the single wild-type peptide served as the input structure for the residue scan, with the Stability/dStability parameters analyzed to provide insights into the importance of each residue for the peptide's structural stability. Subsequently, the complex formed by C3aR and the wild-type peptide was utilized as the input structure for the residue scan. In this case, the Affinity and dAtability parameters were analyzed to assess how mutations on the wild-type peptide might affect its affinity towards the receptor protein C3aR. The residue scan was performed three times to ensure the acquisition of the most stable and reliable data. This comprehensive analysis enables us to gain valuable insights into the structural stability and binding affinity of the peptides, thus guiding the design of potent decoy peptides targeting C3aR.

2.4. Creation of Single Mutation and Double Mutation

A total of 247 single mutations were collected during the residue scan analysis. Following the analysis of Affinity/dAffinity data, 12 single mutations were identified for their notably higher binding affinity with C3aR compared to the wild-type peptide. Subsequently, the Protein Builder tool within MOE was employed to generate the structures of these 12 single mutations, utilizing the wild-type structure as a template. The QuickPrep module in MOE was then applied to these structures to refine them. The QuickPrep procedure involves several steps, including protonation, addition of missing hydrogen atoms, placement of tethers to the active center, fixing of distant atoms, and determination of the overall lowest potential energy configuration for the various states within the system. Furthermore, double mutations were created using the same methodology to explore potential synergistic effects between mutations.

3. Results and Discussions

3.1. C3aR and C3a interaction

In the recent paper elucidating the complex structure of the C3aR-C3a receptor and ligand, Cryo-EM technology was utilized, and the resulting structure can be accessed in the Protein Data Bank under the PDB code 8i9L. Using Pymol software, we extracted both the C3aR receptor and C3a ligand by identifying the involved residues. To analyze the binding affinities and docking modes between the wildtype C3aR and C3a receptor-ligand, we employed the HDock website. By inputting the receptor and ligand into the site, the system generated various predictions/models of the binding, assessing bond strengths and distances between specific residues.

The evaluation of HDock results involved several key scores, including docking scores, confidence scores, and ligand RMSD. Among the c3a-C3aR models generated, the 1st model (see Figure 1A for structure) has a docking score of -461.96 kcal/mol, indicating a highly stable and strongly binding interaction. Furthermore, it exhibited a confidence score of 0.998, indicating a high level of reliability and accuracy in the predicted model. The ligand RMSD for this model was 0.34, suggesting a relatively small deviation from the reference model, thereby affirming the accuracy of the predicted binding configuration. Figure 1B shows detailed 2D representation of the binding interaction, highlighting the residues from C3aR involved in the binding site, and Table S1 lists the strength of interactions between involved residues from C3a and C3aR. Notably, our focus shifted to 13 key residues in C3a (residues

DOI: 10.54254/2753-8818/59/20241372

63-77), including Leu643, Arg64, Arg65, Gln66, His67, Ala68, Arg69, Ala70, Ser71, His72, Leu73, Gly74, Leu75, Ala76, and Arg77. These residues were targeted for mutations to enhance the binding between C3aR and C3a. Analysis revealed that three residues possess nonpolar side chains, two have polar side chains, and the remaining two have electrically charged side chains (basic).

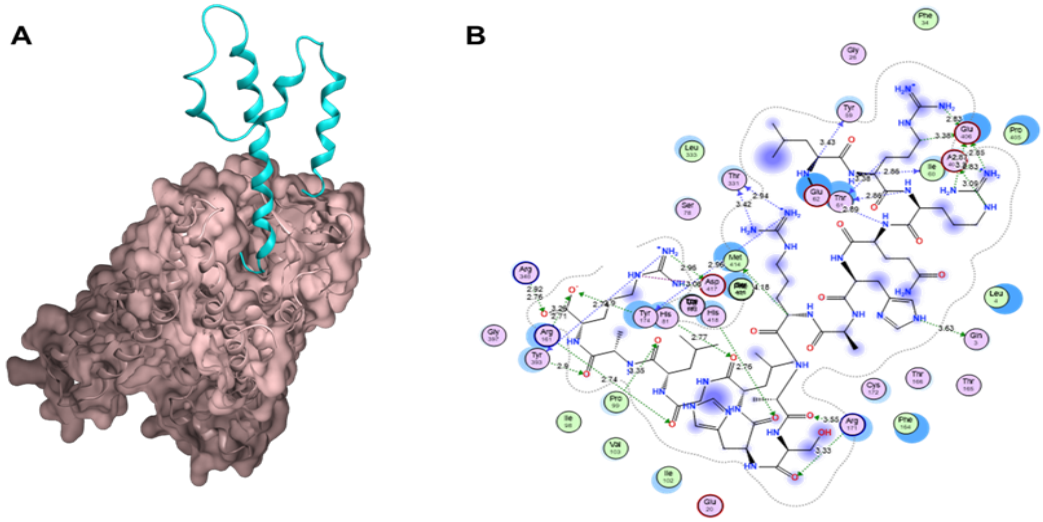

Figure 1. 1st Model of C3aR and C3a from HDock (this study). **A**, surface overview of binding of C3a with C3aR, the ligand C3a is shown in blue, and receptor C3aR is shown in brown. **B**, Detailed 2D representation of the binding interaction, highlighting the residues from C3aR involved in the binding site.

Comparison with prior research utilizing Cryo-EM technology verified the accuracy of our computational approach (Figure 2). Overlapping residues identified in both studies confirm the precision of the HDock algorithm. For instance, residues such as H81, R161, Y174, R340, R393, D417, and H418 in C3aR were identified in both studies as part of the active site. Additionally, residues Gly74, Leu75, and Ala76 in C3a were found to form hydrophobic contacts with specific residues in C3aR, further validating the accuracy of our computational method. Moreover, the computational approach enabled the identification of specific non-bonded and hydrophobic contacts between residues, enhancing our understanding of the molecular interactions. Overall, the alignment of findings from computational and experimental approaches underscores the reliability and accuracy of computational algorithms in studying protein-protein interactions and complex structures.

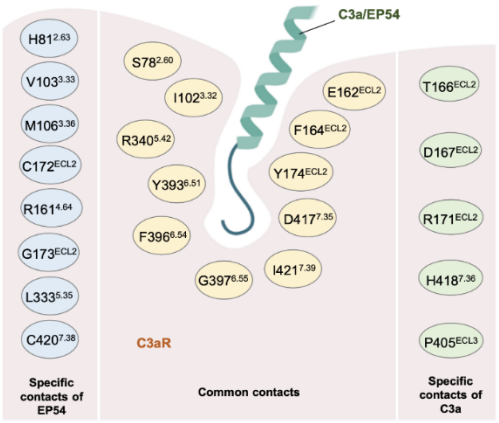

Figure 2. C3aR and C3a binding details. From Cry-EM structure, PDB ID: 8i9l. The figure was adopted from work by Yadav, Yadav, et al. [12].

DOI: 10.54254/2753-8818/59/20241372

3.2. Stability check

Understanding the stability of a protein structure is crucial for elucidating the biophysics of the protein complex and provides insights into the interactions between residues within the ligand. We initiated our analysis by creating a wild-type peptide spanning residues 63 to 77 using C3a as a template and subsequently tested the effect of mutations on stability using the residue scan module of MOE. Analyzing (Supporting information Table S2) reveals that residues A70, H72, and G74 in the C3a ligand exhibit improved stability upon mutation, as indicated by the deeper blue colors. Conversely, residues L63, R69, L73, and L75 are likely to exhibit poorer stability following mutation, as evidenced by the red-colored cells. Notably, three of these residues are Leu, suggesting that the Leu side chain may already contribute effectively to stability. Therefore, mutating these Leu residues may weaken stability within the protein complex.

3.3. Single mutation

After identifying the key residues involved in the binding between C3aR and C3a, spanning residues 63-77 in C3a, we proceeded to perform mutations on these residues to initiate our peptide design process. We utilized the Molecular Operating Environment (MOE) software for this purpose. Each residue from 63-77 was individually selected, and the residue scan function in MOE was employed to analyze how the binding would be affected if the selected residue were replaced by any of the other 19 amino acids. This analysis was crucial in determining which residues could be mutated to strengthen the binding between the receptor and ligand. The focus primarily lay on the affinity and dAffinity data provided by MOE. In Table 1, dAffinities represent the comparison of binding quality and strength of bonds with mutated ligands compared to the original unmutated wildtype ligand C3a. A more negative dAffinity value is indicated by a redder color, suggesting a stronger affinity compared to the wildtype ligand, signifying that the mutation improved the ligand's strength in bonds and binding affinities. The highlighted cells, shown in extra red and bolded font, denote mutations with dAffinities that particularly stood out or were exceptionally strong. Analyzing the table reveals that residues A68, A70, G74, and A76 exhibit more red cells, indicating a higher probability of stronger affinities once mutated. And the dAffinity result aligns with the dStability result.

Table 1. dAffinity table from residue scan of wild-type peptide to C3aR.

mutation	arg64	arg65	gln66	his67	ala68	arg69	ala70	ser71	his72	leu73	gly74	leu75	ala76	arg77
A	-0.72	0.32	2.96	5.54	0.00	5.09	0.00	-0.11	4.12	3.44	-0.56	8.40	0.00	7.46
C	-0.69	-1.10	2.67	-1.31	2.09	3.19	-0.48	-2.55	4.65	2.29	-1.52	4.32	-0.85	5.82
D	-1.89	2.26	-0.18	1.44	-0.97	1.34	-0.68	0.70	3.33	1.74	-1.07	7.66	-0.39	5.54
E	-4.02	1.74	-4.22	-3.06	-3.03	2.26	-6.13	-0.60	1.43	-0.36	-4.36	0.45	-3.91	9.09
F	-3.47	-1.65	1.21	-0.75	**-10.34**	-1.41	-0.43	-4.33	3.19	2.28	-2.55	0.18	**-7.44**	-0.26
G	-1.16	1.91	2.84	-0.49	-4.72	5.78	2.50	0.15	5.42	-0.99	0.00	10.49	3.46	8.70
H	-4.24	2.62	-3.11	0.00	-4.90	4.11	-1.23	-1.95	0.00	6.45	**-7.17**	1.84	-6.99	1.57
I	2.46	2.51	3.11	4.71	1.45	3.28	-6.27	0.49	3.62	1.63	-5.62	1.02	-4.04	2.10
K	1.62	-0.07	3.49	-1.71	4.50	-0.02	**-7.71**	0.75	4.80	-0.59	-2.70	-1.16	-6.93	4.43
L	-3.82	-3.16	3.01	0.08	-0.59	0.63	-2.54	-2.24	0.64	0.00	-3.68	0.00	-0.54	1.57
M	-1.15	-3.64	-0.91	0.40	-2.09	1.51	-2.38	-2.74	-1.57	-0.63	-5.33	0.62	-4.34	2.36
N	-2.92	0.29	3.58	1.37	-0.62	2.66	-3.27	0.87	1.33	0.38	-4.34	2.44	-3.22	3.59
P	-3.68	-0.40	3.74	2.46	1.60	5.17	1.58	1.69	5.27	0.88	-3.74	4.09	-0.67	5.07
Q	-1.49	-0.72	0.00	-0.30	3.67	1.75	-6.75	-0.27	-1.20	1.53	**-7.35**	-0.18	-5.68	6.47
R	0.00	0.00	0.34	-1.69	-2.45	0.00	-6.59	-2.83	0.49	-2.32	**-9.76**	2.57	**-12.24**	0.00
S	-2.17	4.30	4.97	4.96	2.28	6.35	-1.05	0.00	5.30	5.31	-2.15	4.10	-2.07	8.07
T	-2.06	3.36	2.08	2.95	1.48	3.12	-3.70	-0.77	3.53	1.69	-1.92	3.58	0.08	4.38
V	-2.11	-0.57	4.33	3.42	0.94	4.79	-0.01	0.83	5.80	2.57	-1.34	2.73	**-7.32**	3.55
W	-3.37	-3.09	-3.75	-2.90	0.94	-1.88	-0.84	-4.70	-1.29	5.52	-6.79	-1.44	3.50	-1.91
Y	1.39	3.17	0.06	-1.58	-2.14	-2.25	-2.30	-1.41	-1.65	-3.22	-3.86	3.34	**-10.34**	0.29

The dAffinity data indicates how closely the mutated binding/affinity resembles that of the wildtype residue. Thus, mutations with a dAffinity of less than -7 were selected from the 247 mutations performed on the 13 residues. To ensure accuracy and precision, three trials of this process were conducted. Combining the mutations with a dAffinity of less than -7 (12 mutations in Table 2), it was observed that certain residues, specifically residues 74 (Glycine) and 76 (Alanine), had multiple mutations with a

DOI: 10.54254/2753-8818/59/20241372

dAffinity of less than -7. This indicates their potential significance in strengthening the binding between C3aR and C3a.

Table 2. Selected 12 single mutations with stronger binding affinity compared to wild-type peptide.

No.	mutation	Affinity	dAfffinity
1	Wild	-109.88	0
2	A68F	-119.96	-9.56
3	A70Q	-111.39	-7.43
4	A70K	-111.45	-7.71
5	S71W	-116.25	-8.80
6	G74H	-122.80	-7.18
7	G74Q	-123.32	-7.71
8	G74R	-125.48	-9.87
9	A76F	-120.63	-7.44
10	A76R	-125.30	-11.64
11	A76W	-123.95	-9.82
12	A76V	-120.51	-7.32
13	A76Y	-123.53	-10.34

3.4. Docking of screened single mutation

Upon identifying the 13 peptides exhibiting the highest affinity scores post-mutation, our investigation progressed to modeling the resultant changes in residue composition within the C3a ligand. Initially, we focused our attention on residues 64-77 of the C3a protein, recognized for their pivotal role in ligand-receptor interactions. By excluding extraneous residues and isolating residues 63-77 in the ligand, we prepared the protein file for analysis within the Molecular Operating Environment (MOE) software. Utilizing MOE's QuickPrep function, we optimized the ligand's structure by addressing missing hydrogen atoms, establishing tethers to the active center, rectifying distant atoms, and refining the overall energy configuration. Subsequently, employing the protein builder function, we systematically altered the amino acid composition of the target residue to align with the desired mutations outlined in our data. With the mutated residue now embodying a novel peptide configuration, we introduced it into the HDock Server for docking simulations with the C3aR receptor. The HDock Server facilitated the assessment of binding scores and confidence levels, affording visualizations of the mutated peptide's interactions with the C3aR receptor. These analyses provided crucial insights into the peptide's potential efficacy as an antagonist or agonist, guiding further exploration in therapeutic development.

Table 3 summarizes the mutations with significantly low dAffinity values obtained from both trials, consolidating the findings from the previous two tables. These mutations were subjected to docking simulations with the C3aR receptor using the HDock server to assess their binding strength and confidence levels. Therefore, Table 3 presents docking scores and confidence scores instead of Affinity and dAffinity. Among the mutations listed in Table 3, four mutations stood out for their exceptionally strong bindings, as determined by the HDock Server. These highlighted mutations are as follows: G74H, A76F, A76W, and A76Y. These mutations demonstrated the strongest bindings between the mutated C3a ligand and the C3aR receptor, indicating their potential as promising candidates for further investigation and therapeutic development.

DOI: 10.54254/2753-8818/59/20241372

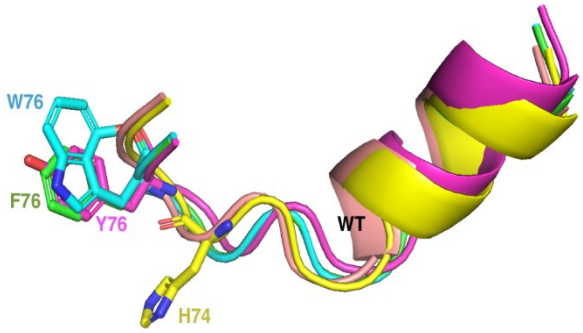

Figure 3. Structure alignment of selected 4 single mutations with wild-type. This is a figure that shows the interaction between the C3a and C3aR proteins and the bigger gray block is the C3aR receptor whereas the smaller blue chain presented in the its cartoon figure is the C3a (with the residues from residue 63-77).

Upon closer examination of the four point mutations—G74H, A76F, A76W, and A76Y—it is evident that these mutations occur at either residue 74 or residue 76 within the C3a ligand. (See Figure 3). Notably, our previous stability check revealed that mutations at these two residues do not destabilize the overall structure of the peptide. The significance of these mutations becomes apparent when considering the characteristics of the amino acids involved. Glycine (Gly) and Alanine (Ala) possess small side chains. However, upon mutation to larger and bulkier amino acids such as Histidine (His), Phenylalanine (Phe), Tryptophan (Trp), and Tyrosine (Tyr), there is a discernible increase in binding affinity. This observation suggests that residues 74 and 76 may play a crucial role in the binding site with the C3aR receptor. The transition from small side chain amino acids to larger, bulky residues likely enhances interactions with the receptor, potentially due to increased steric hindrance and improved complementarity of binding interfaces.

When examining the binding of G74H with C3aR (Figure 4A), glycine possesses a simple side chain with only three molecules, histidine introduces a ring structure. This additional ring structure plays a crucial role in enhancing binding affinity. Specifically, the histidine ring forms three additional bonds with residues on the C3aR receptor, including H418, S78, and I421. Additionally, the switch from a hydrophobic glycine side chain to a positively charged histidine side chain enables the formation of ionic bonds, further reinforcing the binding between the ligand and the receptor. It is noteworthy that all of these bonds are in close proximity, with distances less than 4 units. This close proximity suggests strong interactions between the mutated ligand and the receptor. The binding analysis of A76W, shown in Figure 4B, reveals insights into the role of tryptophan (W) in protein-ligand interactions. Tryptophan stands out among amino acids due to its unique side chain, which features two aromatic rings and exhibits hydrophobic properties. In Figure 4B, it is apparent that the distances between the bonds and residue 76W typically fall within the range of 3 to 4 units. This suggests that the aromatic rings of tryptophan play a crucial role in facilitating close-range interactions with neighboring residues on the C3aR receptor. Moreover, the relatively larger size of tryptophan, coupled with its two aromatic rings, provides a greater number of interaction sites with residues from C3aR within a 5-unit radius. This abundance of interaction sites increases the likelihood of forming stronger and more numerous bonds, further enhancing the binding affinity between the ligands and the protein. It is important to note that tryptophan, despite its hydrophobic nature, does not participate in ionic bonding. Instead, its hydrophobic properties contribute to the formation of stable hydrophobic interactions within the binding interface.

DOI: 10.54254/2753-8818/59/20241372

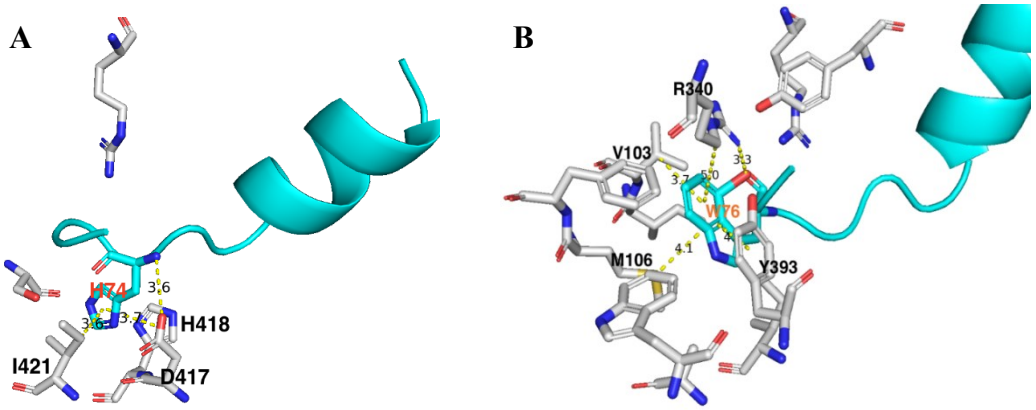

Figure 4. Binding details of G74H (A) and A76W (B) mutation with C3aR. And the lines are the bonds that the mutation has formed with the C3aR receptor (the gray parts) and the numbers on the dotted lines show you the distance of those bonds.

The analysis of A76Y binding to C3aR, as depicted in Figure 5A, provides valuable insights into the role of tyrosine (Y) in protein-ligand interactions. Tyrosine shares similarities with tryptophan in terms of its hydrophobic nature, making it conducive to forming stable hydrophobic interactions within the binding interface. While tryptophan features two aromatic rings, tyrosine possesses only one aromatic ring, with the second ring being replaced by a hydroxyl (OH) group. Upon closer examination, it becomes evident that the introduction of the hydroxyl group does not confer the same benefits as the aromatic ring present in tryptophan. In fact, the bonds observed in the A76Y mutation are longer compared to those in the A76W mutation, indicating weaker interactions between the ligand and the receptor. Furthermore, while the hydroxyl group theoretically offers the potential for hydrogen bonding interactions, its presence does not appear to significantly contribute to the binding affinity between the ligand and the receptor. In Pymol simulations, the hydroxyl group did not form any close or strong bonds, suggesting limited utility in enhancing binding interactions. In the A76F binding analysis (as shown in Figure 5B), phenylalanine (F) emerges as another hydrophobic mutation, akin to the preceding residue 76 mutations. Like tyrosine (Y), phenylalanine features a single aromatic ring in its side chain, albeit lacking the hydroxyl group present in tyrosine. Despite the structural similarity between phenylalanine and tyrosine, phenylalanine exhibits fewer functional groups within its side chain. However, it is worth noting that the absence of the hydroxyl group does not necessarily impede the formation of strong bonds with the C3aR receptor. Upon closer examination of the A76F mutation, it becomes apparent that the bonds formed are shorter in distance compared to those observed in the A76Y mutation. This suggests a potential for stronger interactions between phenylalanine and the residues of the C3aR receptor.

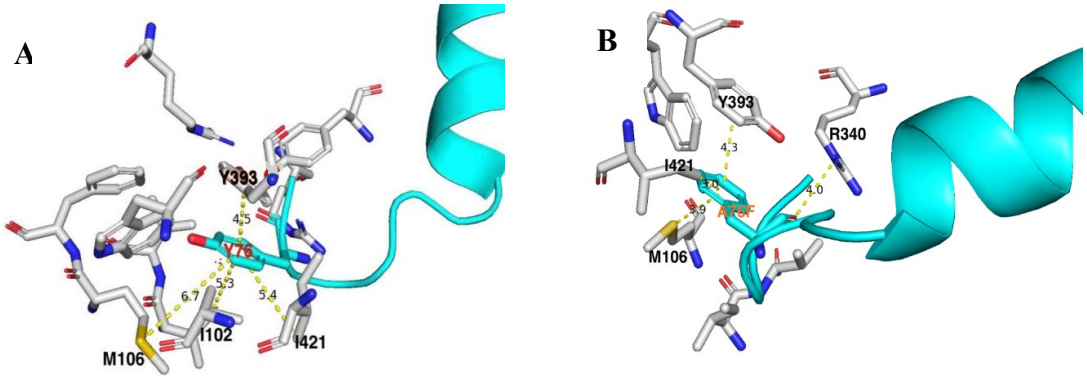

Figure 5. Binding details of A76Y (**A**) and A76F (**B**) mutation with C3aR. This is the same as the last figure where it shows you the mutated residue 76 and the distance and the bonds formed from it.

DOI: 10.54254/2753-8818/59/20241372

3.5. Double mutation

Given the significant impact observed with mutations at residue 76, particularly in conjunction with the G74H mutation, we proceeded to explore the potential synergistic effects of double mutations. Leveraging the promising outcomes of the A76F, A76W, and A76Y mutations, we paired each of these with the G74H mutation to create three double mutations in the C3a ligand. Table 3 presents a comprehensive overview of these double mutations, along with corresponding scores obtained from HDock results. Notably, all three double mutations exhibit markedly stronger binding affinities compared to the wild-type peptide, as evidenced by substantially lower docking scores. Furthermore, the binding confidence scores for these double mutations have significantly increased to 0.99, surpassing those of both the wild-type peptide and single mutations as documented in Table 3.

Table 3. Generated double mutations and docking result from HDock.

No.	Mutation	Docking Score	Confidence Score
1	Wild Type	-266.59	0.9115
2	G74H_A76F	-392.35	0.9922
3	G74H_A76W	-392.21	0.9922
4	G74H_A76Y	-400.56	0.9934

G74H_A76F Binding Analysis is shown in Figure 6A: Examination of the G74H residue reveals the presence of multiple bonds emanating from this position, albeit with elongated bond distances indicative of moderate strength. Intriguingly, the A76F residue displays only two bonds, both characterized by considerable length. In comparison to the G74H_A76W double mutation, which features fewer bonds for the 76H mutation, the A76W variant exhibits a noteworthy proportion of shorter bonds stemming from its 76W residue. Thus, considering the bonding profile observed, the A76W mutation emerges as a potentially superior choice over the A76F mutation for augmenting binding interactions within the G74H_A76F double mutation. G74H_A76W Binding Analysis is shown in Figure 6B. In contrast to the other two double mutations, a notable distinction is observed in the bonding pattern of the G74H residue within this mutation. Surprisingly, the H74 residue forms only a single bond with the C3aR ligand, contrasting with the multiple bonds observed in the other two mutations, which typically range between 4 and 5. Furthermore, the singular bond in this case is relatively weak, indicated by its distance of 4.9. This disparity suggests a potential deficiency in binding interactions involving the 74H residue. Conversely, the W76 residue, characterized by its aromatic side chain with two rings, demonstrates notable advantages. Bonds originating from this residue exhibit significantly shorter distances, indicative of stronger binding affinities. Moreover, the presence of multiple short bonds stemming from the 74H residue further enhances the binding potential of the W76 residue. These findings underscore the beneficial role of the aromatic side chain in promoting robust binding interactions within the G74H_A76W double mutation. G74H_A76Y Binding Analysis is shown in figure 6C, in line with our observations from the single A76Y mutation analysis, the hydroxide moiety at the terminal end of the tyrosine ring appears to offer limited utility, as evidenced by the absence of ionic bonds formed by this hydroxide group. Moreover, the bonds formed by the 74H residue exhibit similarities to those observed in the G74H_A76W mutation, characterized by multiple bonds albeit of moderate strength. Furthermore, examination of the bonds originating from the aromatic rings in the tyrosine amino acid reveals multiple interactions, albeit with relatively elongated distances, indicating suboptimal bonding strength. This suggests that while the aromatic side chain may contribute to binding interactions, the bonds formed may not be as robust as desired. Overall, the G74H_A76Y double mutation presents a bonding profile similar to that of the G74H_A76W mutation, albeit with slight variations in bond strength and configuration.

DOI: 10.54254/2753-8818/59/20241372

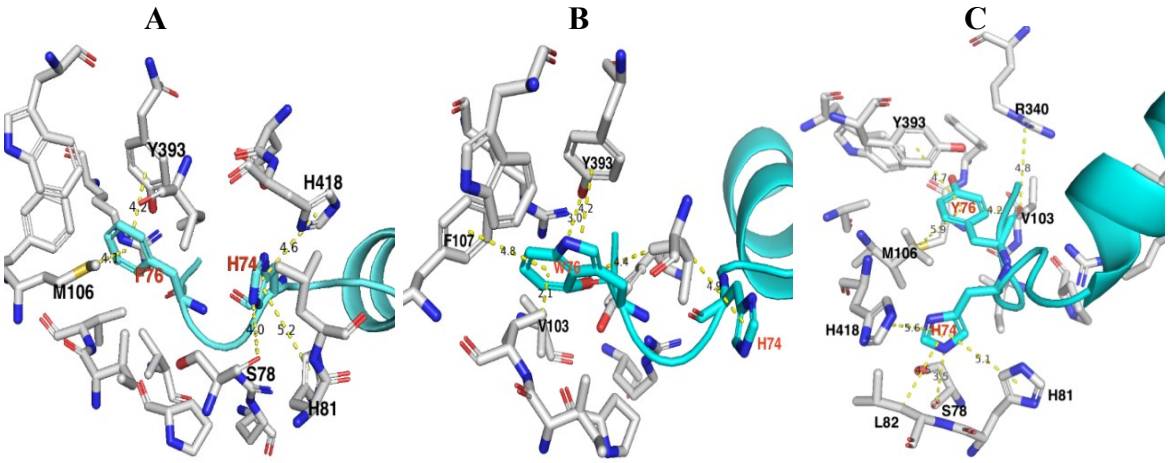

Figure 6. binding of G74H_A76F (A), G74H_A76W (B) and G74H_A76Y (C) to C3aR. This shows the bonds that are formed from the two mutated residues on the C3a protein (74H and 76 mutated residues)

4. Conclusion

Our comprehensive analysis of single and double mutations within the C3a ligand has provided valuable insights into the determinants of binding affinity and interaction patterns with the C3aR receptor. Through meticulous examination of individual mutations (247 total mutations), we identified key residues, particularly at positions 74 and 76, that significantly influence binding dynamics. The G74H mutation emerged as a pivotal contributor to enhanced binding affinity, facilitating the formation of multiple bonds with the C3aR receptor. Additionally, the introduction of bulky amino acids at position 76, such as tryptophan (A76W), yielded further improvements in binding interactions, attributed to the presence of aromatic rings and shorter bond distances.

Furthermore, our investigation into double mutations revealed synergistic effects, particularly when combining the G74H mutation with A76W. This combination resulted in significantly strengthened binding affinity and confidence scores, highlighting the potential for synergistic enhancements in peptide-receptor interactions. However, mutations involving tyrosine (A76Y) and phenylalanine (A76F) residues exhibited comparable or slightly inferior binding characteristics, suggesting a nuanced interplay between residue properties and their impact on binding affinity.

Overall, our research contributes to advancing our understanding of inflammation biology and offers promising avenues for the development of targeted therapies for inflammatory diseases. By unraveling the molecular intricacies of the C3a ligand-receptor complex, we aim to pave the way for the development of novel anti-inflammatory therapeutics with improved efficacy and specificity, ultimately benefiting patients afflicted with chronic inflammatory disorder.

References

[1] Afshar-Kharghan, V. (2017). The role of the complement system in cancer. *The Journal of clinical investigation*, *127*(3), 780-789.

[2] Corcoran, J. A., & Napier, B. A. (2022). C3aR plays both sides in regulating resistance to bacterial infections. *PLoS Pathogens*, *18*(8), e1010657.

[3] Dalakas, M. C., Alexopoulos, H., & Spaeth, P. J. (2020). Complement in neurological disorders and emerging complement-targeted therapeutics. *Nature Reviews Neurology*, *16*(11), 601-617.

[4] Ricklin, D., & Lambris, J. D. (2013). Complement in immune and inflammatory disorders: pathophysiological mechanisms. *The Journal of Immunology*, *190*(8), 3831-3838.

[5] Wang, Y., Zhang, H., & He, Y.-W. (2019). The complement receptors C3aR and C5aR are a new class of immune checkpoint receptor in cancer immunotherapy. *Frontiers in immunology*, *10*, 439560.

DOI: 10.54254/2753-8818/59/20241372

[6] Espinosa-Riquer, Z. P., Segura-Villalobos, D., Ramírez-Moreno, I. G., Pérez Rodríguez, M. J., Lamas, M., & Gonzalez-Espinosa, C. (2020). Signal transduction pathways activated by innate immunity in mast cells: translating sensing of changes into specific responses. *Cells*, *9*(11), 2411.

[7] Wende, E., Laudeley, R., Bleich, A., Bleich, E., Wetsel, R. A., Glage, S., & Klos, A. (2013). The complement anaphylatoxin C3a receptor (C3aR) contributes to the inflammatory response in dextran sulfate sodium (DSS)-induced colitis in mice. *PLoS One*, *8*(4), e62257.

[8] Halai, R., Bellows-Peterson, M. L., Branchett, W., Smadbeck, J., Kieslich, C. A., Croker, D. E., Cooper, M. A., Morikis, D., Woodruff, T. M., & Floudas, C. A. (2014). Derivation of ligands for the complement C3a receptor from the C-terminus of C5a. *European Journal of Pharmacology*, *745*, 176-181.

[9] Hawksworth, O. A., Li, X. X., Coulthard, L. G., Wolvetang, E. J., & Woodruff, T. M. (2017). New concepts on the therapeutic control of complement anaphylatoxin receptors. *Molecular immunology*, *89*, 36-43.

[10] Zhang, Y.-y., & Ning, B.-t. (2021). Signaling pathways and intervention therapies in sepsis. *Signal Transduction and Targeted Therapy*, *6*(1), 407.

[11] Yadav, M. K., Maharana, J., Yadav, R., Saha, S., Sarma, P., Soni, C., Singh, V., Saha, S., Ganguly, M., & Li, X. X. (2023). Molecular basis of anaphylatoxin binding, activation, and signaling bias at complement receptors. *Cell*, *186*(22), 4956-4973. e4921.

[12] Yadav, M. K., Yadav, R., Sarma, P., Maharana, J., Soni, C., Saha, S., Singh, V., Ganguly, M., Saha, S., & Khant, H. A. (2023). Structural insights into agonist-binding and activation of the human complement C3a receptor. *bioRxiv*, 2023.2002. 2009.527835.

[13] Yan, Y., Tao, H., He, J., & Huang, S.-Y. (2020). The HDOCK server for integrated protein–protein docking. *Nature protocols*, *15*(5), 1829-1852.

Supplementary information

Table S1: List of residues from C3aR involved in the binding site from HDock (this study).

Receptor-C3aR	Ligand-C3a	Distance (Å)
H81	L73	2.767
R161	F74	2.744
R161	R77	2.714
T165	Q3	2.769
D167	Q3	2.541
Y174	R69	2.962
Y174	R77	2.904
T331	R69	2.938
R340	R77	2.764
R393	A76	2.897
R393	R77	2.743
D404	R65	2.83
E406	R64	2.83
E406	R65	2.851
D417	R77	2.783
H418	H72	2.756

DOI: 10.54254/2753-8818/59/20241372

Table S2: dStability table from residue scan of wild-type peptide. Each residue was mutated to 19 amino acids to stability test.

Mutation	Leu63	Arg64	Arg65	Gln66	His67	Ala68	Arg69	Ala70	Ser71	His72	Leu73	Gly74	Leu75	Ala76	Arg77
A	2.12	0.37	1.15	1.06	0.72	0.00	2.20	0.00	0.27	0.53	2.26	-0.01	2.02	0.00	1.67
C	1.72	0.20	1.62	0.76	0.63	0.55	2.00	0.74	0.37	0.43	2.17	0.12	2.15	0.84	1.55
D	2.11	0.76	0.84	1.09	1.10	0.94	2.82	1.11	1.32	0.95	2.54	0.12	2.47	1.08	2.49
E	1.71	0.84	0.70	0.91	0.29	0.62	2.02	0.85	1.11	0.51	1.94	0.39	1.85	1.70	2.13
F	0.87	-0.49	0.08	0.56	-0.69	0.39	0.24	-0.94	0.02	-0.76	1.48	-0.90	0.54	-0.37	-0.65
G	2.34	0.96	2.33	1.93	1.47	1.48	2.96	1.61	0.72	0.98	3.90	0.00	2.86	1.60	2.38
H	1.64	0.66	1.07	1.63	0.00	1.44	1.85	0.49	0.59	0.00	1.76	-0.58	1.99	0.65	1.40
I	0.43	-0.22	0.17	0.57	-0.66	-0.14	0.61	-0.84	0.31	-0.32	1.25	-1.04	0.67	0.49	0.46
K	1.82	1.10	1.18	1.01	1.04	1.44	1.54	-0.30	0.97	0.12	1.70	-0.38	1.22	1.06	0.49
L	0.00	-0.26	-0.26	0.07	-0.76	-0.33	0.55	-1.08	-0.18	-0.87	0.00	-0.89	0.00	0.01	0.31
M	1.47	-0.05	0.37	0.31	-0.42	-0.10	1.03	-0.22	0.40	-0.13	1.63	-0.44	0.92	0.04	0.23
N	1.67	0.42	1.08	0.51	0.64	0.77	2.10	0.62	0.40	0.67	2.31	0.20	2.01	1.12	1.70
P	2.34	1.45	2.35	2.53	1.27	1.82	2.80	1.76	1.08	0.84	2.77	-0.01	2.03	1.10	1.06
Q	1.51	0.56	0.90	0.00	0.13	0.31	1.46	-0.72	0.65	0.56	2.11	0.59	1.74	0.84	1.43
R	0.72	0.00	0.00	1.03	-0.03	1.05	0.00	-0.25	-0.31	-0.38	0.89	-0.92	0.29	0.14	0.00
S	2.50	0.38	1.79	1.53	0.96	0.75	2.43	0.83	0.00	0.61	2.59	0.46	2.47	1.13	1.78
T	0.82	0.20	0.56	0.86	0.56	0.62	1.67	0.16	0.35	0.43	1.82	0.26	1.63	0.70	1.08
V	0.72	-0.11	0.59	0.94	-0.05	0.19	1.08	-0.32	-0.15	-0.06	1.52	-0.34	0.73	0.62	1.00
W	1.39	-0.70	0.46	-0.06	-0.36	0.09	0.38	-1.57	-0.39	-1.25	0.81	-1.69	0.73	-0.08	-0.84
Y	0.80	-0.18	0.14	0.28	-0.21	0.17	0.91	-0.53	-0.02	-0.13	1.59	-1.31	0.88	-0.49	-0.31

Table S3: Score from HDock docking of 13 peptides to C3aR

No.	Mutation	Docking Score	Confidence Score
1	Wild	-266.59	0.9115
2	A68F	-263.82	0.9069
3	A70Q	-275.3	0.9246
4	A70K	-226.75	0.8227
5	S71W	-276.71	0.9265
6	G74H	-309.7	0.9606
7	G74Q	-299.66	0.9523
8	G74R	-292.6	0.9454
9	A76F	-334.36	0.9756
10	A76R	-288.5	0.941
11	A76W	-334.01	0.9754
12	A76V	-284.82	0.9368
13	A76Y	-328.41	0.9726